Analysis of finite-time regulation property of biomolecular PI controller

doi: https://doi.org/10.1007/s11768-020-0017-2

Control Theory and Technology

Analysis of finite-time regulation property of biomolecular PI controller

Peng RONG [1], Takashi NAKAKUKI [2†],

1.*Major of Interdisciplinary Informatics, Kyushu Institute of Technology;*

2.*Department of Intelligent and Control Systems, Kyushu Institute of Technology*

Abstract:

In practical applications of dynamic DNA nanotechnology, a biomolecular controller is required for maintaining the operation of the molecular actuator at a desired condition based on the information from molecular sensors. By making use of the DNA strand displacement mechanism as a "programming language" in the controller design, a biomolecular PI controller has been proposed. However, this PI control system has been verified only at the simulation level, and a theoretical regulation analysis is still required. Accordingly, in this study, we perform a rigorous regulation analysis of the biomolecular PI control system. Specifically, we theoretically prove that the output signal approaches the target level at a quasi-steady state. To this end, we apply the concept of finite-time regulation property to the biomolecular PI control system.

Keywords: Molecular robotics, Biomolecular reaction system, PI controller, Finite-time regulation property

*DOI https://doi.org/10.1007/s11768-018-****-**

1 Introduction

Recent advances in nanotechnology have enabled the realization of practical molecular systems, such as molecular robots [1]. A molecular robot is comprised of a molecular sensor that can receive stimuli from the environment, and a molecular actuator that can act on the environment. As in mechatronics robots, a feedback control system that links information from a molecular sensor to a molecular actuator is required in molecular robots to achieve practical tasks [2]. It should be noted that information transmission between a molecular sensor/actuator and a feedback circuit must be performed with signaling molecules. Therefore, the concentration of the signaling molecule is the physical quantity that represents the "signal" flowing in the control system [3]. As a result, a control mechanism needs to be designed by molecular computing, and a control circuit needs to be implemented as a biomolecular reaction system.

In practical applications of molecular robots, a biomolecular controller is required for maintaining the operation of the molecular actuator at a desired condition based on the information from the molecular sensor. This is a so-called regulator, which tries to adjust the concentration of the specific signaling molecule sent to the actuator to a reference level [3]. In recent years, DNA computing has been widely used as a methodology for designing molecular feedback controllers. Especially, the DNA strand displacement (DSD) mechanism is useful as a "programming language" in DNA computing, and its computational universality has been proved theoretically [4]. In previous studies [5], three basic elements have been constructed using the DSD mechanism, namely the gain, summation, and integration elements, and a biomolecular PI controller has been rationally designed [6]. It has also been shown that the proportional and integral gains, which are the controller parameters, can be adjusted by changing the molecular structures of the DNA molecules. Nevertheless, the realization of a derivative element using the DSD mechanism has been a long-standing problem. However, a design method for pseudo-derivative elements has been devised, which enables the development of a PID con-

†Corresponding author.

E-mail: nakakuki@ces.kyutech.ac.jp. Tel.: +81-948-29-7716; fax: +81-948-29-7709.

This work was supported by JSPS KAKENHI Grant Number 17K06500.

troller [7]. In addition, a switching mechanism using the DSD mechanism has been proposed to realize a molecular sliding mode controller [8].

On the other hand, a regulator designed using the DSD mechanism is a high-dimensional nonlinear system, so it is extremely difficult to analyze the stability of the closed-loop system theoretically. In particular, it is known that the regulation operation whereby the output signal follows the reference level appears at a quasi-steady state, so the stability analysis of the equilibrium point of the system has no meaning [3]. In fact, the biomolecular PI control system has been verified only at the simulation level, and its theoretical regulation analysis is required. This is a common problem that applies to other systems, including biomolecular PID and sliding mode controllers.

In this study, we perform a rigorous regulation analysis of the biomolecular PI control system. Specifically, we theoretically prove that the output signal matches the target level at the quasi-steady state. To this end, we introduce the concept of finite-time regulation property [9]. First, through numerical simulation, we confirm that the normal regulation observed in the biomolecular PI control system can be achieved only during a limited period of time. Next, we convert the ordinary differential equation of the biomolecular PI control system into a two-time scale model in accordance with the transformation proposed in [9] and employ the singular perturbation theory. Finally, we evaluate the behavior of the solution of the fast system analytically and show that the system has a finite-time regulation property. Because the mathematical model of the PI control system is quite high-dimensional, its analysis is performed by using computer algebra software. This paper presents the outline of the analysis procedure, the results of the PI control system, and the detailed analysis method using a simple model example.

2 Preliminaries

2.1 System description of biomolecular PI controller

The biomolecular PI controller can be designed by a combination of three basic reactions, namely degradation, annihilation, and catalysis, which provide the cornerstone of the design of biomolecular circuits [5]. Its abstract reaction mechanism is described as follows [6]:

Plant (first-order lag element) :

$$U^+ \xrightarrow{k_1} U^+ + Y^+, \quad Y^+ \xrightarrow{k_2} \phi, \tag{1}$$
$$U^- \xrightarrow{k_1} U^- + Y^-, \quad Y^- \xrightarrow{k_2} \phi, \tag{2}$$

Error calculation:

$$R^+ \xrightarrow{k_c} R^+ + E^+, \quad E^+ \xrightarrow{k_d} \phi, \tag{3}$$
$$R^- \xrightarrow{k_c} R^- + E^-, \quad E^- \xrightarrow{k_d} \phi, \tag{4}$$
$$Y^+ \xrightarrow{k_c} Y^+ + E^-, \quad E^- \xrightarrow{k_d} \phi, \tag{5}$$
$$Y^- \xrightarrow{k_c} Y^- + E^+, \quad E^+ \xrightarrow{k_d} \phi, \tag{6}$$

Proportional element:

$$E^+ \xrightarrow{k_p k_c} E^+ + U^+, \quad U^+ \xrightarrow{k_d} \phi, \tag{7}$$
$$E^- \xrightarrow{k_p k_c} E^- + U^-, \quad U^- \xrightarrow{k_d} \phi, \tag{8}$$

Integral element:

$$E^+ \xrightarrow{k_c} E^+ + I^+, \tag{9}$$
$$E^- \xrightarrow{k_c} E^- + I^-, \tag{10}$$
$$I^+ \xrightarrow{k_i k_c} I^+ + U^+, \quad U^+ \xrightarrow{k_d} \phi, \tag{11}$$
$$I^- \xrightarrow{k_i k_c} I^- + U^-, \quad U^- \xrightarrow{k_d} \phi, \tag{12}$$

Annihilation mechanism:

$$U^+ + U^- \xrightarrow{k_a} \phi, \tag{13}$$
$$R^+ + R^- \xrightarrow{k_a} \phi, \tag{14}$$
$$Y^+ + Y^- \xrightarrow{k_a} \phi, \tag{15}$$
$$E^+ + E^- \xrightarrow{k_a} \phi, \tag{16}$$
$$I^+ + I^- \xrightarrow{k_a} \phi, \tag{17}$$

where U^+, U^-, Y^+, Y^-, R^+, R^-, E^+, E^-, I^+, and I^- denote specific DNA strands. The symbol ϕ represents a "waste" DNA strand generated through an irreversible reaction; the symbol ϕ is used for all individual waste DNA strands for convenience. The right arrow ($\rightarrow$) denotes a biomolecular reaction, and the parameters k_1, k_2, k_c, k_d, k_p, k_i, and k_a shown on the arrows represent the rate constants. The addition symbol ($+$) in the left- and right-hand sides denote binding and unbinding reactions, respectively. It should be noted that a molecular system cannot deal with real numbers in $\mathbb{R}$ explicitly because the state variables are positive molecular concentrations. To solve this problem, two types of DNA strands that store positive and negative state values are defined, and the real number of the signal is calculated as follows:

$$u = u^+ - u^- \tag{18}$$
$$r = r^+ - r^- \tag{19}$$
$$y = y^+ - y^- \tag{20}$$
$$e = e^+ - e^- \tag{21}$$
$$i = i^+ - i^- \tag{22}$$

where u, r, y, e, and i are signals on $\mathbb{R}$, and their superscripts x^+ and x^- denote the concentrations of DNA strands X^+ and X^-, respectively, with $x \in \{u, r, y, e, i\}$ and $X \in \{U, R, Y, E, I\}$. Based on this formalism, the PI control system shown in Fig. 1 can be realized *in vitro*.

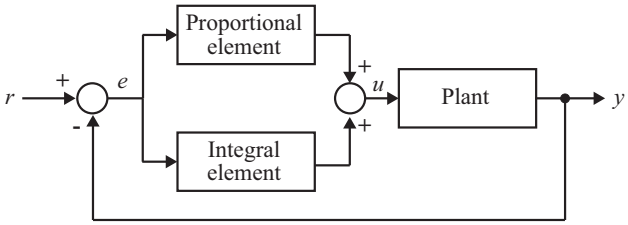

Fig. 1 PI control system defined by Eqs. (1)–(22).

2.2 Implementation using DSD mechanism

The PI control system defined by Eqs. (1)–(17) can be implemented by using the DSD mechanism [6]. For example, the abstract reaction mechanism of "catalysis" described as

$$X^+ \longrightarrow X^+ + Y^+ \tag{23}$$

can be designed at the structural domain level of DNA strands using the computer software Visual DSD (Microsoft Corporation), which is specialized in the design of biomolecular circuits by the DSD mechanism [10], as shown in Fig. 2. This catalysis reaction is comprised of 29 kinds of DNA strands (depicted by a square frame) and 18 biomolecular reactions (depicted by bidirectional arrow of which white head indicates the forward reaction). The DNA strands surrounded by bold square frames have initial concentrations, and the others represent intermediate states generating through a series of reactions. The domain structure of a DNA strand illustrated in the square frame is shown by the notation of Visual DSD (See [1] for details). The mathematical model consists of a 29-dimensional ordinary differential equation with input x^+ and output y^+. As a result, the overall PI control system is a 255-dimensional nonlinear differential equation consisting of 329 biomolecular reactions described as

$$\dot{\xi} = \psi(\xi), \quad \xi(0) = \xi_0, \tag{24}$$

where $\xi \in D_\xi \subset \mathbb{R}^{255}$ is a state vector whose elements are the concentrations of DNA strands, and $\psi : D_\xi \to \mathbb{R}^{255}$ is a nonlinear function characterized by the mass action law. The graphical view of the abstract reaction mechanism, schematic views of the detailed DSD reactions, and parameter values and initial concentrations and their Matlab (Mathworks, Inc.) codes are available in [6] or from the Visual DSD website [11].

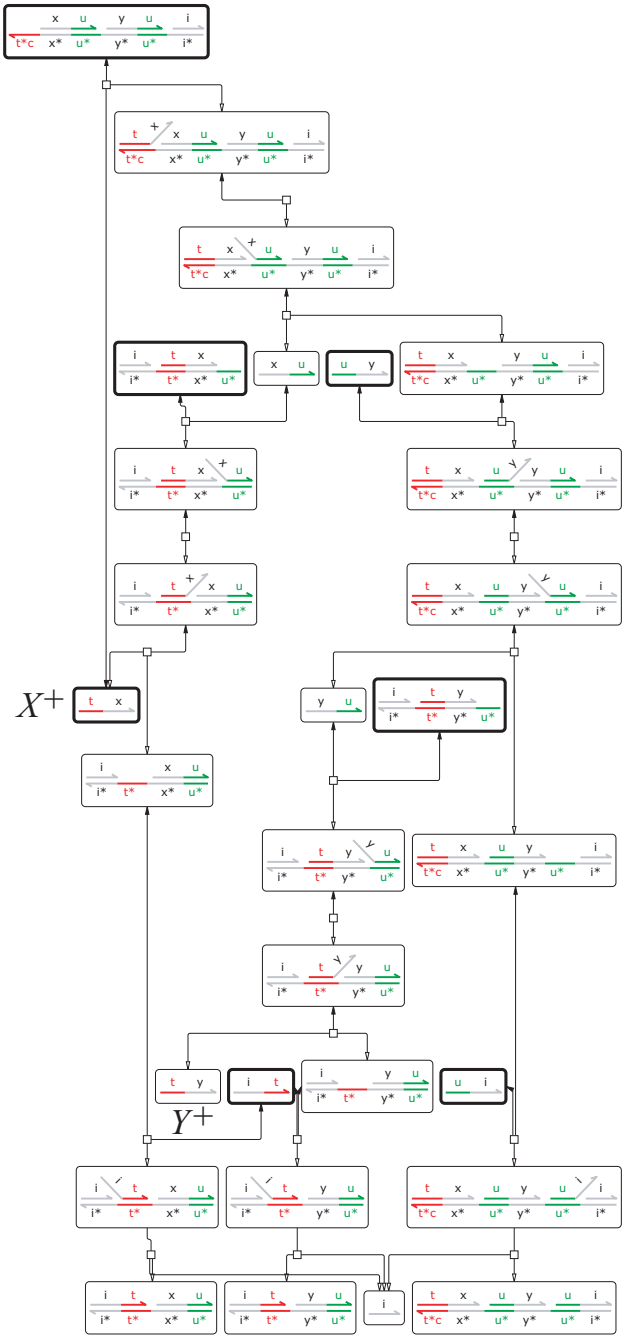

Fig. 2 Detailed reaction scheme of catalysis (illustrated by Visual DSD with the compilation mode "detailed").

Fig. 3 shows a simulation result of the PI control system (24) with proportional gain $k_p = 10$ and integral gain $k_i = 10$ executed by Visual DSD. The rate constants are $k_1 = 0.2\ \mathrm{s}^{-1}$, $k_2 = 0.1\ \mathrm{s}^{-1}$, $k_c = k_d = 0.0008\ \mathrm{s}^{-1}$, and $k_a = 0.01\ \mathrm{nM}^{-1}\mathrm{s}^{-1}$. At first glance, it seems that the regulation of output y to the reference r was successful.

Remark 1 It is noted that, as with conventional PI control, the proportional and integral gains must be adjusted appropriately to obtain the desired response.

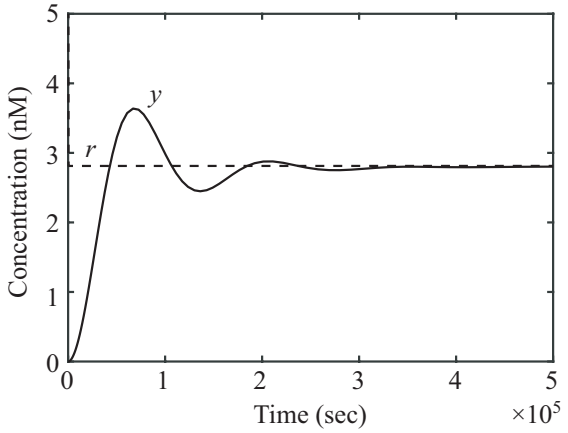

Fig. 3 Simulation of PI control system.

2.3 Problem statements

It is important to note that the regulation shown in Fig. 3 is not achieved at the steady state. In fact, as shown in Fig. 4, if the simulation is performed for a longer time, the regulation collapses, and the output y transitions to the real steady state. In other words, in the biomolecular PI control system, regulation is a transient phenomenon emerging while reaching the steady state, and is different from the "regulation" obtained as time t tends to ∞, i.e., in the context of classical control theory. Therefore, it is unclear whether the PI control system is really a regulator. More precisely, whether the output y is theoretically guaranteed to approach reference r, at least during a certain period of time.

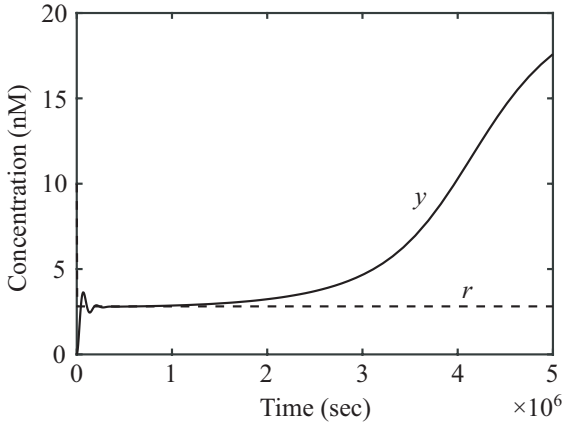

Fig. 4 Long-term simulation of PI control system.

3 Results

The regulation of a molecular feedback system, including biomolecular PI controllers, needs to be evaluated in the framework of the finite-time regulation property (see Definition 1). Because it is impossible to verify the whole PI control system described by the 255-dimensional differential equation due to space limitations, the analysis procedure of the finite-time regulation property is conducted following the steps below.

Step 1 Classify 255 kinds of DNA strands of the PI control system (24) into 48 fuel and 207 signal strands in accordance with Definition 2. ♢

Step 2 Transform the PI control system (24) into a two-time-scale model. Because the system does not include (i) fuel-to-fuel binding and (ii) sequential and irreversible hybridization among signal strands, all requirements of the conversion given by Assumption 1 in [9] are satisfied. In accordance with the procedure for the transformation to a two-time-scale model (see Theorem 1 in [9] for details), the PI control system (24) is transformed into 48-dimensional slow and 207-dimensional fast systems as follows:

$$\dot{x}=f(x,z,\varepsilon)=A_f(z)x+b_f(z,\varepsilon),\ x(0)=x_0\in B_x, \quad (25)$$
$$\varepsilon\dot{z}=g(x,z,\varepsilon)=A_g(x)z+\varepsilon b_g(z),\ z(0)=z_0\in B_z, \quad (26)$$

where $x = [x_1, ..., x_{48}]^T \in D_x \subset \mathbb{R}^{48}$ and $z = [z_1, ..., z_{207}]^T \in D_z \subset \mathbb{R}^{207}$ are the "dimensionless" slow and fast states, respectively, $B_x = \{x \in D_x | \sum_{i=1}^{48} x_i = 1\}$ and $B_z = \{z \in D_z | \sum_{i=1}^{207} z_i = 1\}$ are the sets of initial states, $A_f : D_z \to \mathbb{R}^{48\times 48}$ and $A_g : D_x \to \mathbb{R}^{207\times 207}$ are matrix-valued affine functions, $b_f : D_z \times \mathbb{R} \to \mathbb{R}^{48}$ is comprised of linear and/or quadratic terms with $b_f(0, \varepsilon) = 0$, $b_g : D_z \to \mathbb{R}^{207}$ comprises quadratic terms with $b_g(0) = 0$, and ε is a sufficiently small positive constant. ♢

Before describing Step 3, we give an example that roughly explains why a biomolecular system created by the DSD mechanism can be converted into a two-time-scale model through Steps 1 and 2.

Example 1 (Concept of two-time-scale modeling) Consider a simple binding-unbinding reaction of $X_1 + X_2 \rightleftharpoons X_3$. The detailed reaction process can be modeled as follows:

$$\dot{\xi}_1 = -k_f\xi_1\xi_2 + k_r\xi_3,\ \xi_1(0) = \xi_{1_0}, \quad (27)$$
$$\dot{\xi}_2 = -k_f\xi_1\xi_2 + k_r\xi_3,\ \xi_2(0) = \xi_{2_0}, \quad (28)$$
$$\dot{\xi}_3 = k_f\xi_1\xi_2 - k_r\xi_3,\ \xi_3(0) = \xi_{3_0}, \quad (29)$$

where ξ_1, ξ_2, and ξ_3 are the concentrations of X_1, X_2, and X_3, respectively. The rate constants k_f and k_r are the binding and unbinding rate constants, respectively. We assume that the input signal ξ_1 is transmitted into the signal strand ξ_3 whereas ξ_2 contributes to providing the fuel for driving the circuit. Hence, their initial concentrations are given under the condition satisfying $0 \leq \xi_{1_0} \ll \xi_{2_0}$ and $0 \leq \xi_{3_0} \ll \xi_{2_0}$, indicating that X_2 is a fuel strand, and X_1 and X_3 are signal strands.

Let the total concentrations of signal strands and fuel strands be $T_s = \xi_1(0) + \xi_3(0)$ and $T_f = \xi_2(0)$, respectively. We normalize ξ_i $(i = 1, 2, 3)$ as

$$\bar{\xi}_1 = \frac{\xi_1}{T_s};\ \bar{\xi}_2 = \frac{\xi_2}{T_f};\ \bar{\xi}_3 = \frac{\xi_3}{T_s}, \tag{30}$$

and normalize the time variable as $t_r = k_f T_s t$. Then, we obtain the following two-time-scale model:

$$\frac{d\bar{\xi}_2}{dt_r} = -\bar{\xi}_1\bar{\xi}_2 + \frac{k_r}{k_f T_f}\bar{\xi}_3,\ \bar{\xi}_2(0) = 1, \tag{31}$$

$$\varepsilon\frac{d\bar{\xi}_1}{dt_r} = -\bar{\xi}_1\bar{\xi}_2 + \frac{k_r}{k_f T_f}\bar{\xi}_3,\ \bar{\xi}_1(0) = \bar{\xi}_{1_0}, \tag{32}$$

$$\varepsilon\frac{d\bar{\xi}_3}{dt_r} = \bar{\xi}_1\bar{\xi}_2 - \frac{k_r}{k_f T_f}\bar{\xi}_3,\ \bar{\xi}_3(0) = \bar{\xi}_{3_0}, \tag{33}$$

where $\varepsilon = T_s/T_f \ll 1$ is a dimensionless positive parameter, and the initial concentrations are given by $(\bar{\xi}_{1_0}, \bar{\xi}_{3_0}) \in \{(\bar{\xi}_1, \bar{\xi}_3) \in \mathbb{R}^2 | \bar{\xi}_1 + \bar{\xi}_3 = 1\}$. It is noted that the new states $\bar{\xi}_1$ and $\bar{\xi}_3$ are always finite even if ε tends to 0 ($T_s \to 0$). This fact is easily confirmed as follows: from (27) and (29), for all $t \geq 0$, we have

$$\dot{\xi}_1 + \dot{\xi}_3 \equiv 0 \ \to\ \xi_1(t) + \xi_3(t) \equiv T_s \ \to\ \bar{\xi}_1 + \bar{\xi}_3 \equiv 1. \tag{34}$$

The positivity with $\bar{\xi}_1 \geq 0$ and $\bar{\xi}_3 \geq 0$ leads to $\bar{\xi}_1 \leq 1$ and $\bar{\xi}_3 \leq 1$ for all $t \geq 0$ independent of ε. Therefore, it is safe to assume that this two-time-scale model is also a singular perturbation model.

Fig. 5 shows the simulation result for the original system (27)–(29) and the transformed system (31)–(33), where $k_f = 5 \times 10^{-5}$ nM^{-1}s^{-1}, $k_r = 1.2$ s^{-1}, $\xi_{1_0} = 1$ nM, $\xi_{2_0} = 10000$ nM, and $\varepsilon = 1 \times 10^{-4}$. It is observed that the states $\bar{\xi}_1$ and $\bar{\xi}_3$ respond much faster than $\bar{\xi}_2$, indicating that the system has the two-time-scale property. ♢

Remark 1 This two-time-scale property is somewhat non-intuitive, which is rather strange considering the original description (27)–(29). However, if the state variables are evaluated in terms of the relative amount of change from their respective initial concentrations, a small change (e.g., 0.3 nM) of ξ_2 from the large initial concentration (e.g., 10,000 nM) in Fig. 5 becomes almost negligible in the dynamics of $\bar{\xi}_2$. As a result, the state variable $\bar{\xi}_2$ can be regarded as a slow-mode variable. It is noteworthy that the normalization (30) depends on T_f and T_s, which are determined by the initial concentrations of the fuel and signal strands, respectively. ♢

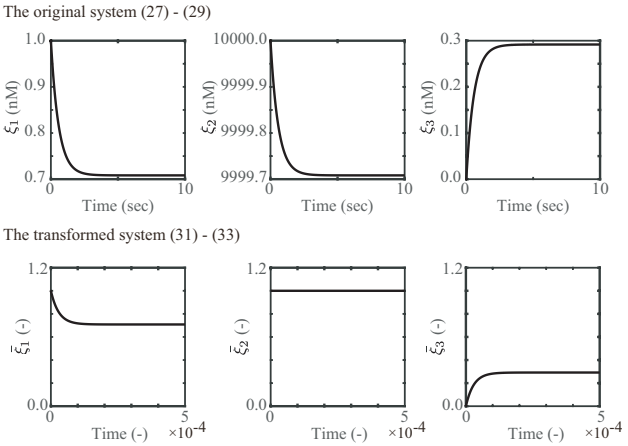

Fig. 5 Simulated results for Example 1.

Next, we continue the description of the steps of the analysis.

Step 3 Investigate the trajectories of the z-system on the invariant manifold by analytically solving $g(x, z, 0) = 0$. Because, as we can easily check, $A_g(x)$ of (26) has some zero eigenvalues and no eigenvalue with a positive real part for all D_x, Lemma 2 in [9] indicated that there exists an exponentially stable invariant manifold for the boundary layer system with $\varepsilon = 0$. By using a computer algebra system, such as Mathematica (Wolfram Research), we can verify that the relation $r = y$ is satisfied on the manifold, so Theorem 3 in [9] indicates that the PI control system (24) has the finite-time regulation property. ♢

The following simple "gain element" example roughly explains the analysis procedure through Steps 1, 2, and 3.

Example 2 (Outline of analysis procedure) Consider the following abstract reaction mechanism

$$X_1 + X_2 \rightleftharpoons X_3 \rightleftharpoons X_4 \rightleftharpoons X_5 + X_6. \tag{35}$$

The detailed reaction process can be modeled as

$$\begin{aligned}
\dot{\xi}_1 &= -k_{f_1}\xi_1\xi_2 + k_{r_1}\xi_3,\\
\dot{\xi}_2 &= -k_{f_1}\xi_1\xi_2 + k_{r_1}\xi_3,\\
\dot{\xi}_3 &= k_{f_1}\xi_1\xi_2 - k_{r_1}\xi_3 - k_2(\xi_3 - \xi_4),\\
\dot{\xi}_4 &= k_2(\xi_3 - \xi_4) + k_{f_3}\xi_5\xi_6 - k_{r_3}\xi_4,\\
\dot{\xi}_5 &= -k_{f_3}\xi_5\xi_6 + k_{r_3}\xi_4,\\
\dot{\xi}_6 &= -k_{f_3}\xi_5\xi_6 + k_{r_3}\xi_4,
\end{aligned} \tag{36}$$

where ξ_i $(i = 1, ..., 6)$ denotes the concentration of DNA strand X_i, and coefficients k_{f_i}, k_{r_i} $(i = 1, 3)$, and k_2 denote the binding, unbinding, and branch migration rate constants, respectively. This reaction system generates output strand X_6 upon the input of strand X_1, where X_2 and X_5 are considered fuel strands and the others are considered signal strands. It has been reported that system (36) can function as a gain element [12]. Through Steps 1 and 2, we obtain

$$A_f(z)=\begin{bmatrix} -\dfrac{k_{f_1}z_1}{k_f} & 0 \\ 0 & -\dfrac{k_{f_3}z_4}{k_f} \end{bmatrix}, \tag{37}$$

$$b_f(z)=\begin{bmatrix} \dfrac{k_{r_1}}{k_fT_f}z_2 \\ \dfrac{k_{r_3}}{k_fT_f}z_3 \end{bmatrix}, \tag{38}$$

$$A_g(x)=\begin{bmatrix} -\dfrac{k_{f_1}x_1}{k_f} & \dfrac{k_{r_1}}{k_fT_f} & 0 & 0 \\ \dfrac{k_{f_1}x_1}{k_f} & -\dfrac{k_{r_1}+k_2}{k_fT_f} & \dfrac{k_2}{k_fT_f} & 0 \\ 0 & \dfrac{k_2}{k_fT_f} & -\dfrac{k_2+k_{r_3}}{k_fT_f} & \dfrac{k_{f_3}x_2}{k_f} \\ 0 & 0 & \dfrac{k_{r_3}}{k_fT_f} & -\dfrac{k_{f_3}x_2}{k_f} \end{bmatrix}, \tag{39}$$

where $b_g(z) = 0$, $\varepsilon = T_s/T_f$, $x = [x_1\ x_2]^T = [\xi_2/T_f\ \ \xi_5/T_f]^T$, and $z = [z_1\ z_2\ z_3\ z_4]^T = [\xi_1/T_s\ \xi_3/T_s\ \xi_4/T_s\ \xi_6/T_s]^T$ are the dimensionless state variables, and $T_s = \xi_1(0) + \xi_3(0) + \xi_4(0) + \xi_6(0)$, $T_f = \xi_2(0) + \xi_5(0)$, $k_f = \max\{k_{f_1}, k_{f_3}\}$, and $t_r = T_sk_ft$ are the dimensionless time variables. In this case, we can see that $A_g(x)$ is a compartment matrix. It is noted that $A_g(x)$ has a zero eigenvalue, which is also the Frobenius eigenvalue, related with the mass conservation law among the four signal strands.

Now, for a given $x(0) = x_0$, consider a non-singular transformation T that transforms $A_g(x_0)$ into a Jordan form:

$$\Lambda := TA_g(x_0)T^{-1} = \begin{bmatrix} O & 0 \\ 0 & A_2 \end{bmatrix}, \tag{40}$$

where $A_2 \in \mathbb{R}^{3\times3}$ is a Hurwitz matrix. Then, the change in coordinate can be performed as follows:

$$\begin{bmatrix} p \\ q \end{bmatrix} \triangleq Tz, \tag{41}$$

transforms z-system into the following form:

$$\varepsilon \begin{bmatrix} \dot{p} \\ \dot{q} \end{bmatrix} = \begin{bmatrix} 0 & 0 \\ 0 & A_2 \end{bmatrix} \begin{bmatrix} p \\ q \end{bmatrix} + T \begin{bmatrix} -k'_{f_1}\delta_{x_1} & 0\,0 & 0 \\ k'_{f_1}\delta_{x_1} & 0\,0 & 0 \\ 0 & 0\,0 & k'_{f_3}\delta_{x_2} \\ 0 & 0\,0 & -k'_{f_3}\delta_{x_2} \end{bmatrix} T^{-1} \begin{bmatrix} p \\ q \end{bmatrix}, \tag{42}$$

where $p \in \mathbb{R}$, $q \in \mathbb{R}^3$, $A_2 \in \mathbb{R}^{3\times3}$, $T \in \mathbb{R}^{4\times4}$, $\delta_{x_i}(t) = x_i(t) - x_i(0)$ for $i = 1, 2$, and $k'_{f_i} = k_{f_i}/k_f$ for $i = 1, 3$. By numerically solving (42) with $\varepsilon = 0$ under the condition that $k_{f_i} = 5 \times 10^{-4}$ nM^{-1}s^{-1}, $k_{r_i} = 0.7$ s^{-1} $(i = 1, 3)$, and $k_2 = 1$ s^{-1} for the kinetic constants; $\xi_2(0) = 2 \times 10^4$ and $\xi_5(0) = 1 \times 10^4$ nM for fuel strands; and $\xi_1(0) = 1.0$, $\xi_3(0) = 0$, $\xi_4(0) = 0$, and $\xi_6(0) = 0$ nM for signal strands, it is confirmed that A_2 is Hurwitz with $\lambda = -1.97,\ -0.98,\ -0.31$, and the relation $z_4/z_1 \simeq x_1(0)/x_2(0)$ is satisfied for the trajectories on the manifold h. In fact, by directly solving the steady-state equation of the z-system (26) with (39), we can also obtain the following relations analytically:

$$h = \left\{ q \in \mathbb{R}^3 \,\middle|\, \begin{bmatrix} p \\ q \end{bmatrix} = Tz, \right. \\ \left. z_4 = \frac{k_{f_1}k_{r_3}}{k_{f_3}k_{r_1}}\frac{x_1}{x_2}z_1, z_2 = \frac{k_{f_1}T_fx_1}{k_{r_1}}z_1, z_2 = z_3 \right\}. \tag{43}$$

By substituting the three equations of (43) into the x-system (25) with (37)–(38), we analytically obtain the following quasi-steady state model:

$$\dot{\delta}_x = F(\delta_x, p_0, 0, 0) \equiv 0, \tag{44}$$

where $\delta_x(t) = x(t) - x_0$, and $p_0 = z_1(0) + z_2(0) + z_3(0) + z_4(0)$. Therefore, we conclude from Theorems 2 and 3 in [9] that for all $t_b > 0$, there exist positive constants k^{**} and ε^{**} such that for all $w_0 \in \Omega_w$ and $\varepsilon \in (0, \varepsilon^{**})$,

$$\left| z_4(t) - \frac{k_{f_1}k_{r_3}}{k_{f_3}k_{r_1}}\frac{x_1(0)}{x_2(0)}z_1(t) \right| \le k^{**}\varepsilon,\ \forall t \ge t_b, \tag{45}$$

which implies that the gain between the input ξ_1 and the output ξ_6 is adjusted by the ratio of fuels $\xi_2(0)/\xi_5(0)$. This result is consistent with the estimate given in [12]. Interestingly, the gain is determined by the ratio of the "initial" concentrations between fuel strands. We illustrate the simulation result of the gain element, indicating that the gain is approximately 2 $(= 0.623/0.312)$, which is in agreement with the ratio of $\xi_1(0)/\xi_2(0) = 2$ (Fig. 6). ♢

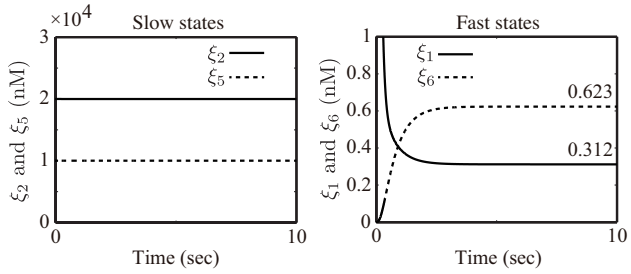

Fig. 6 Simulation result of gain element (36).

4 Conclusions

In this study, we evaluated the regulation property of the biomolecular PI control system by examining Steps 1–3. Because it has been confirmed that the system has finite-time regulation property, the tracking of the output signal to the reference signal observed in the simulation has been theoretically validated.

Furthermore, we analyzed the control performance of the biomolecular PI control system designed by DNA reactions. However, it might be possible to apply the finite-time regulation property to other biomolecular reaction systems, such as a control system designed in the field of synthetic biology.

References

[1] Y. Sato, Y. Hiratsuka, I. Kawamata, S. Murata, and S. M. Nomura. Micrometer-sized molecular robot changes its shape in response to signal molecules. *Science Robo.*, Vol. 2, No. 4, pp. 1–10, 2017.

[2] S. Murata, A. Konagaya, S. Kobayashi, H. Saito, and M. Hagiya. Molecular robotics: A new paradigm for artifacts. *New Generation Computing*, Vol. 31, No. 1, pp. 27–45, 2013.

[3] T. Nakakuki and J. Imura. Molecular governor: Dna feedback regulator for molecular robotics. *SICE J of Cont Meas and Syst Int*, Vol. 9, No. 2, pp. 60–69, 2016.

[4] D. Soloveichik, G. Seelig, and E. Winfree. Dna as a universal substrate for chemical kinetics. *PNAS*, Vol. 107, No. 12, pp. 5393–5398, 2010.

[5] K. Oishi and E. Klavins. A biomolecular implementation of linear i/o systems. *IET Syst. Biol*, Vol. 5, pp. 252–260, 2011.

[6] B. Yordanov, J. Kim, R. L. Petersen, A. Shudy, V. V. Kulkarni, and A. Phillips. Computational design of nucleic acid feedback control circuits. *ACS Synt Biol*, Vol. 3, No. 8, pp. 600–616, 2014.

[7] N. M. G. Paulino, M. Foo, J. Kim, and D. G. Bates. Pid and state feedback controllers using dna strand displacement reactions. *IEEE Control Systems Letters*, Vol. 3, No. 4, pp. 805–810, 2019.

[8] R. Sawlekar, F. Montefusco, V. V. Kulkarni, and D. G. Bates. Implementing nonlinear feedback controllers using dna strand displacement reactions. *IEEE Trans. NanoBiol.*, Vol. 15, No. 5, pp. 443–454, 2016.

[9] T. Nakakuki and J. Imura. Finite-time regulation property of dna feedback regulator. *Automatica*, Vol. 114, pp. 1–10, 2020.

[10] M. R. Lakin, S. Youssef, F. Polo, S. Emmott, and A. Philleps. Visual dsd: a design and analysis tool for dna strand displacement systems. *Bioinformatics*, Vol. 27, pp. 3211–3213, 2011.

[11] Visual dsd (microsoft corporation). *https://www.microsoft.com/en-us/research/publication/visual-dsd-a-design-and-analysis-tool-for-dna-strand-displacement-systems/.*

[12] S. Kobayashi, K. Yanagibashi, K. Fujimoto, K. Komiya, and M. Hagiya. Analog dna computing devices toward the control of molecular robots. In *Workshop on Self-organization in Swarm of Robots: from Molecular Robots to Mobile Agents*, 2014.

Appendix

Definition 1 (Finite-time regulation property [9]) Consider a DNA feedback regulator system given by

$$\begin{aligned} \dot{\xi} &= \psi_{\rm dfr}(\xi),\ \xi(0) = \xi_0, \\ y_p &= c_{\rm dfr}\xi, \end{aligned} \tag{a1}$$

for a time period $t \in [0, t_1]$, where $\xi = [r\ \xi_{\bar{r}}^T]^T \in D_\xi \subset \mathbb{R}^\zeta$ is the state vector that is comprised of the reference signal $r \in \mathbb{R}$ and other strands $\xi_{\bar{r}} \in \mathbb{R}^{\zeta-1}$, and $y_p \in \mathbb{R}$ is the output signal. $\psi_{\rm dfr} : D_\xi \to \mathbb{R}^\zeta$ is a nonlinear vector-valued function characterized by the mass action law, and $c_{\rm dfr} \in \mathbb{R}^{1\times\zeta}$ is a constant vector. System (a1) is said to have the finite-time regulation property if, for each of all $e > 0$ and $t_b \in (0, t_1)$, there exists a set of initial state $\Omega_\xi \subset D_\xi$ such that for all $\xi_0 \in \Omega_\xi$,

$$|y_p(t) - r(t)| \le e,\ \forall t \in [t_b, t_1]. \tag{a2}$$

Definition 2 (Fuel and signal strands [9]) Consider the biomolecular reaction system described by

$$\dot{\xi} = \psi(\xi),\ \ \xi(0) = \xi_0, \tag{a3}$$

where $\xi \in D_\xi \subset \mathbb{R}^\zeta$ is a state vector of which elements are concentrations of DNA strands, and $\psi : D_\xi \to \mathbb{R}^\zeta$ is a nonlinear function characterized by the mass action law. Let $I_{\rm fuel}$ and $I_{\rm signal}$ be index sets such that $\xi_i(0) \gg \xi_j(0)$, $\forall i \in I_{\rm fuel}$, $\forall j \in I_{\rm signal}$ and $I_{\rm fuel} \bigcup I_{\rm signal} = \{1, ..., \zeta\}$. The symbol X_i is termed a signal strand for $i \in I_{\rm signal}$, and a fuel strand for $i \in I_{\rm fuel}$.

Peng RONG received his M.S. degree from Kyushu Institute of Technology, Japan, in 2020.

Takashi NAKAKUKI received his B.E. and M.S. degrees from Sophia University, Japan, in 1997 and 1999, respectively. From April 1999 to March 2003, he worked at Sony Corporation. He obtained his Ph.D. degree in mechanical engineering from Sophia University, Tokyo, Japan, in 2006. He was subsequently employed at RIKEN from April 2006 to March 2009, and at the Department of Mechanical Systems Engineering, Kogakuin University, from April 2009 to March 2013. In April 2013, he joined Kyushu Institute of Technology, where he is currently a Professor in the Department of Intelligent and Control Systems.